

Development and Mechanical Properties of Compacted Graphite Cast Iron (CGI) Suitable for Exhaust System Pipes.

Abstract: This research focuses on developing compacted graphite iron (CGI) and its mechanical properties for the production of exhaust system parts. Theoretical and practical failure analysis were carried out on selected exhaust system parts. Based on the failure analysis compacted graphite cast iron was casted. Six different types of CGI term C1 to C6 were produced, incorporating alloying elements such as chromium, aluminum, copper, titanium and nickel in micro amounts. The study also investigated the mechanical properties of CGI, including tensile strength, hardness, and impact resistance, aiming to understand the material's behavior under relevant conditions. These addition alloys aimed to enhance mechanical properties, such as tensile strength, impact resistance, and ductility, which are important for exhaust system materials. Optical microscope was carried out on the produce CGI to check their microstructure. The results from the micrograph shows that CGI of varying microstructure was produce. The results from the mechanical tests show that C4 has the optimum values of 1.5 Megapascal for tensile strength, 615% for ductility, 204 Brinell hardness value of 204 and 35.9 Joule per millimeter square value for impact strength. By analyzing these properties, the study provides valuable insights into the performance and durability of CGI for the production of exhaust system pipes, aiding in the design and selection process for automotive applications.

Keywords: **Compacted Graphite Cast Iron (CGI), Mechanical properties, Exhaust system pipes, Alloying elements, Failure analysis**

1. Introduction:

Compacted Graphite Cast Iron (CGI) is an advanced material that has emerged as a promising alternative to conventional cast iron and other metallic alloys in various engineering applications [1]). The unique microstructure of CGI, characterized by compacted graphite flakes, imparts exceptional mechanical properties, making it a preferred choice for demanding industrial uses [2].

The distinctive feature of CGI lies in its graphite morphology, where the graphite flakes are shorter, thicker, and interconnected, compared to the randomly distributed graphite in gray cast iron [3]). This unique microstructure gives CGI its superior properties, combining the benefits of both gray cast iron and ductile cast iron [4]). As a result, CGI exhibits remarkable tensile strength, excellent thermal conductivity, and improved fatigue resistance, making it a versatile material suitable for a wide range of engineering applications [5])

One area where the exceptional properties of CGI hold significant importance is in the production of exhaust system pipes [6]. In modern automotive and industrial systems, exhaust system pipes are exposed to severe operating conditions[7]. These conditions include high temperatures arising from the combustion process, cyclic thermal loading due to the engine's operation, and exposure to corrosive gases and particles [8]. Additionally, exhaust pipes may encounter mechanical stresses and impacts during vehicle operations[9].

The mechanical properties of a car's exhaust system are critical for its performance, durability, and compliance with environmental regulations[10]. These properties are determined by the materials used, the design, and the manufacturing processes[11]. Some vital mechanical properties which is significant to car exhaust are strength and durability, thermal resistance, impact strength and ductility [12]. The exhaust system must withstand the stresses caused by thermal expansion, vibrations, and external forces without failing and the material must resist fatigue failure due to cyclic thermal and mechanical loading[13].

To ensure the reliable and efficient performance of exhaust systems, it is imperative to select materials that can withstand these harsh conditions over an extended service life [14]. Traditional materials like gray cast iron have been used in exhaust system pipes due to their cost-effectiveness and reasonable thermal conductivity [15]. However, they often fall short in meeting the ever-increasing demands for improved performance and durability [16] .

The need for more robust materials with enhanced mechanical properties, superior corrosion resistance, and increased thermal conductivity has prompted the exploration of alternatives, with CGI emerging as a compelling solution [17]. Its ability to provide high tensile strength, excellent thermal conductivity, and good resistance to corrosion makes it an ideal candidate for exhaust system pipes, which are vital components in automotive and industrial machinery [18].

This research focuses on investigating the mechanical properties of CGI specifically for its application in exhaust system pipes. By comprehensively understanding the material's behavior under relevant conditions, including high temperatures, cyclic thermal loading, and corrosive environments, valuable insights can be obtained to optimize CGI's performance in exhaust system applications. The findings from this study will aid in the design and selection process for automotive and industrial exhaust systems, contributing to the development of more efficient, durable, and sustainable engineering solutions.

2. Experimental method

2.1 Materials and alloy formulation

The materials used to produce alloys include cast iron engine block scraps, rotary furnaces, crucible pots, and alloying elements. Six different types of CGI were developed with different alloying elements ranging from chromium, aluminum, copper, and nickel. These as-cast (produced) CGI, were tagged C1, C2, C3, C4, C5, and C6. These alloys were added in a micro amount of about 0.1% - 0.5%. for every 10kg of melt.

2.2 Charge analysis of CGI

It was done manually based on the charged metallurgical principle of producing CGI. Table 1 show the charging analysis of the alloying elements adding to every 10kg of melt. Factors like chemical composition of charge materials, metallurgical treatment, and ratio of charge materials to inoculants and spheroidizers and to other alloying elements were all considered. The charged ratio was arrived at using Equation 1[19].

$$A = \frac{R - (BM) X (TW)}{PA}$$

(1)

Commented [U1]: Use Equation editor

Where

A is number of alloying elements to be added

R IS required amount

BM is amount in base metal

TW is total weight of the charge and

PA is purity of the alloying elements.

The ratio alloying addition was varied for six different 10kg of charge cast iron materials with

different alloying elements. These were done so as to control the nodularity and graphite growth in order to produce CGI and not gray or ductile cast iron. The CGI produced were labelled C1, C2, C3, C4, C5 and C6.

Table 1. Charge Analysis of Alloying Elements

Sample	Furnace addition alloying elements			Ladle addition alloying element		
C1	Al (16mg)	FeSiMg (25mg)	FeSi (34mg)	FeSi (14.5mg)		
C2	FeSi(14.5mg)	FeSiMg (25mg)		FeSi (14.5mg)	Ti (2.5mg)	
C3	Al (25mg)	FeSiMg (25mg)	FeSi(14.5mg)	FeSi (14.5mg)	Ti(2.5mg)	
C4	Al(25mg)	Cu(20mg)	FeCr (15mg)	FeSi(14.5mg)	Ti(2.5mg)	Fe(20g)
C5	Cu(20mg)	FeCr (15mg)	FeSiMg(25mg)	Al(20mg)	Ti(2.5mg)	FeSi(14.5mg)
C6	Cu (20mg)	Fe(10mg),FeCr(15mg)	FeSiMg(25mg)	Al(20mg)	Ti(2.5mg)	FeSi(14.5mg)

2.3. Melting

Rotary furnace of 40 Kg capacity was used for the melting. The required quantities of the charging materials were weighed using weighing balance and charged into the furnace. cast iron engine scraps were first charged and heated to the temperature of 1200°C before the addition of inoculants alloying elements. Nodularizers alloying elements were added in the ladle during tapping. Pouring was done at 1250°C into the ladle.

2.4 Determination of the composition of failed exhaust pipes and the produced CGI

The chemical composition of exhaust pipes of some selected cars and the produced CGI (C1-C6) was determined. The cars whose exhaust were analyzed are Nissan Altima (N11), Toyota corolla (T1), Toyota Highlander jeep (T12), Mitsubishi car (M11), and Mitsubishi outlander (M12). Figure 1 and 2 show some of the exhaust system and CGI that were analyzed using Skyray EDX 3600B energy dispersive, X-ray fluorescence (XRF) spectrometer was used to determine the elemental composition

of C1-C6 and five different exhaust pipes viz-a-vis N11, T11, T12, M11, and M12. X-ray fluorescence is a powerful technique used in a wide variety of elemental composition of various materials [20]. XRF analyzer are widely recognized as a means for accurate, rapid and non-destructive testing [21]. The skyray EDX3600B is a high-end energy dispersive spectrometer with a large sample chamber which support most sample size [22]. It involves the generation of a spark discharge between an electrode and the sample surface which excites the atoms in the sample [23]. As the excited atoms return to their ground state, they emit characteristic wavelengths of light, which are then analyzed to determine the elemental composition of the samples [24].



Figure 1: Exhaust System Parts for failure analysis



Figure 2: CGI produced of size 16mm x 5mm

2.5 Optical microscopy

The microstructural and morphological characterization of CGI produced were done by optical microscopy (OM). The equipment used was ultra-high-resolution field emission Nikon E200 laboratory microscope. The first phase of the process was grinding using aluminum oxides and silicon carbide paper of 220 grades with tap flowing water. While, the second stage was using finer abrasive grinder cover with velvet cloths. The third stage was done which is called lapping, was done to remove any little remaining imperfection in the CGI produced so as to produce a very smooth and mirror-like surface of the material. Finally, the material was etched in nitric acid and nital base mixture before it was viewed under microscope lens at magnification of 100 μm

2.6 Tests for the mechanical properties

2.6.1 Hardness

The hardness test was conducted using the hand-held micro Brinell tester. This conforms to ISO and ASTM E03-18 [25] standard which was used on all metals and alloys on any sample size. The set of tests were performed on C1-C6. The test was done on four occasions and the average was recorded.

2.6.2 Tensile and ductility

Tensile tests were performed on the six samples of CGI produce labeled C1-C6 using the universal testing machine. A material testing system with a load capacity of 50 KN, at a loading speed of 10 rpm and a maximum chuck diameter of 10mm. The test samples were prepared on the lathe machine in cylindrical shapes of 9 mm x 16 mm. The samples were inserted into the chuck and were closed by Allen key to grip them and the samples were pull apart until they broke into pieces. Ductility result is calculated from percentage elongation gotten from the tensile test result.

2.6.3 Impact strength

Impact strength was evaluated on the produce materials labeled C1, C2, C3, C4, C5, and C6. The test was conducted using ASTM standard of dimension 9 mm x 16mm using the Hounsfield balance impact machine. The V-notch impact specimen was clamp into the pendulum chuck and locked with Allen key, the notched side facing the striking edge direction. The pendulum was released at a velocity of 4 m/s with maximum energy of 170 these were done to fracture the materials and the energy absorb by the materials were noted and recorded. Four tests were carried out on each specimen and their average were recorded in joules which is unit of energy.

3.0 Results and Discussion

3.1 Elemental analysis of some exhaust pipes

The chemical composition of exhaust pipes of some selected cars was determined. The results obtained from the analysis were recorded. The results shown in Table 2, revealed that the composition used by Nissan to produce their exhaust pipe/silencer was medium carbon steel with addition some major alloying elements. Chiefly, 18% chromium, 0.258% manganese and .27% nickel were added and other elements were added in micro amount. In the case of Toyota corolla, it was shown clearly, that their exhaust system was made of high carbon steel of 0.55% with other alloying elements added in minor amount. The chromium content of the exhaust was low at 0.0945%. Likewise, the results also reveal that the composition found in Toyota highlander jeep were low carbon steel with other elements like chromium, copper and nickel added in micro amounts. Just like the cast of Toyota corolla, the chromium content of 0.0256% for Toyota highlander was low too. Table 2 also, shown that the constituents of exhaust found in Mitsubishi car were low carbon steel, with

addition of 12% chromium and other elements like silicon, aluminum, nickel was added in little quantity. It was shown that the elements used for the production of exhaust system for Mitsubishi outlanders were found out to be low carbon steel, with 11% chromium and other elements added in minute amount.

Table 2: Chemical Compositions of Some Selected Exhaust Parts

	Fe	C	Si	Cr	Mn	P	Cu	Ni	Al	Mg	Tot
N11	78.8000	0.3700	0.4540	18.3200	0.2580	0.0406	0.0734	0.2170	0.0346	0.1000	98.6700
T11	97.5000	0.5500	0.0128	0.0945	0.1620	0.0218	0.0210	0.0217	0.0594	0.0100	98.4532
T12	97.5000	0.0225	0.0981	0.0256	0.1170	0.0112	0.0074	0.0114	0.0370	0.0010	98.1543
M11	85.6000	0.0405	0.3680	12.0300	0.4400	0.0588	0.2690	0.2290	0.0298	0.0077	99.0728
M12	85.6000	0.0251	0.362	11.9100	0.4430	0.0524	0.2690	0.3390	0.0439	0.0076	98.9213

3.2 Determination of the Composition Analysis of the as- Cast CGI

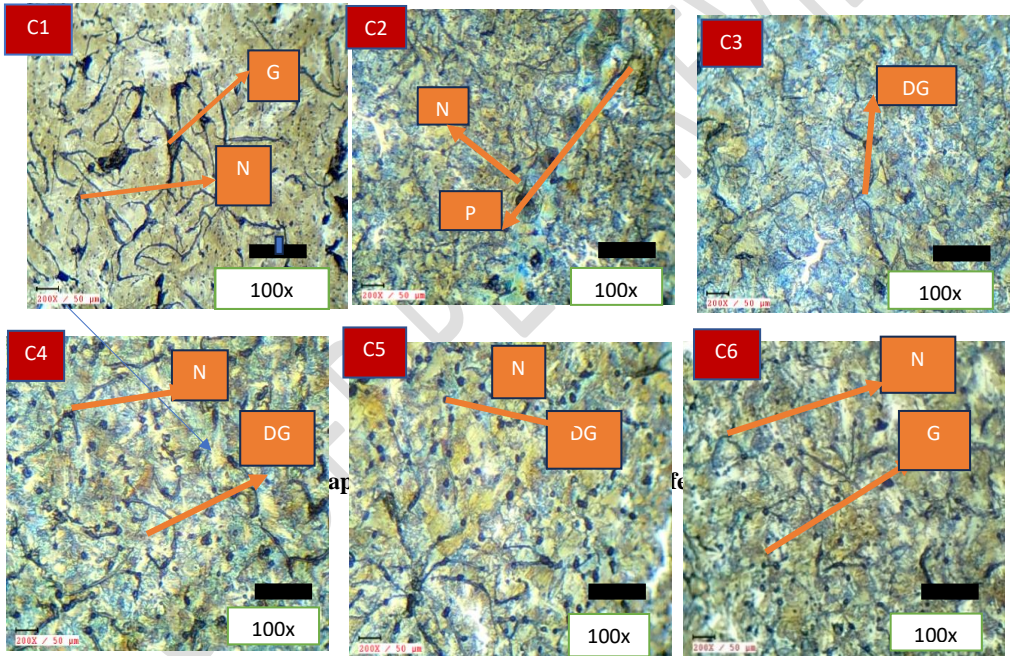
Skyray EDX 3600B energy dispersive X-ray fluorescence spectrometer was used to determine the elemental composition of the six as-cast CGI -C1, C2, C3, C4, C5, and C6 as show in Table 3. The test piece whose surface was ground to ensure flatness was mounted on the sparking point of the spectrometer and the chemical composition was obtained after 40–50 s of operation.

Table 3: Summary Elemental Composition of As-Cast (C1-C6)

	Fe	C	Si	Cu	Cr	Ti	Al	Ni	Mg	S	Mn	Total
C1	93.1000	4.3500	1.5300	0.1610	0.0774	0.0057	0.2090	0.0566	0.0029	0.0953	0.2360	99.8791
C2	92.6000	4.3500	1.8200	0.1820	0.0900	0.0134	0.1630	0.0438	0.0064	0.1390	0.2800	99.7856
C3	92.5000	4.3500	1.8800	0.1920	0.0943	0.0211	0.1610	0.0433	0.0038	0.1350	0.2590	99.9780
C4	92.4000	4.3500	2.0000	0.3450	0.1410	0.0183	0.0307	0.0531	0.0048	0.1320	0.2770	99.8568
C5	92.0000	4.3500	2.2300	0.3590	0.1550	0.017	0.0597	0.1790	0.0082	0.1440	0.2820	99.8923
C6	92.4000	4.3500	2.0200	0.3400	0.1300	0.0374	0.0294	0.0053	0.0053	0.1200	0.2760	99.7994

3.3 Optical microscopy

Figure 3, shows all materials produced contain pearlite and little ferrite but there is a dark graphite which is worm-like in nature, embedded in pearlite and α -ferrite of C1 and C2 and has a microstructural composition towards gray cast iron. Pearlite is hard and brittle because of the increase in cementite ratio compare to α -ferrite according to Garcí et al. 2019 While C3 and C4 microstructure have equal composition of both gray and nodularized cast iron graphite flakes. It is pure CGI and CGI properties fall between the properties of gray and ductile cast iron according to [27]. Lastly, C5 and C6 microstructures are more of ductile graphite composition



N=nodules, DG= distorted graphite, G=graphite, P= pearlite

Figure 3. C1-C6 microstructures under 100 magnifications

3.3 Hardness

Hardness is the ability to withstand surface indentation (localized plastic deformation) and scratching [28]. Under normal conditions the hardness value of gray iron is higher than that of ductile iron and CGI hardness value is expected to be the least [6]. The hardness result from Figure 4 shows that the C-series materials produced are hard (especially at the surface and it might be ductile in the inner core) and might be susceptible to brittle failures during service use. The Brinell hardness values for C1 of 231 and C3 of 218 falls within the standard hardness values for gray cast iron according to (Upadhyay and Saxena, 2020). while C2 and C4 values are CGIs. C5 and C6 hardness values are close to ductile cast iron hardness values.

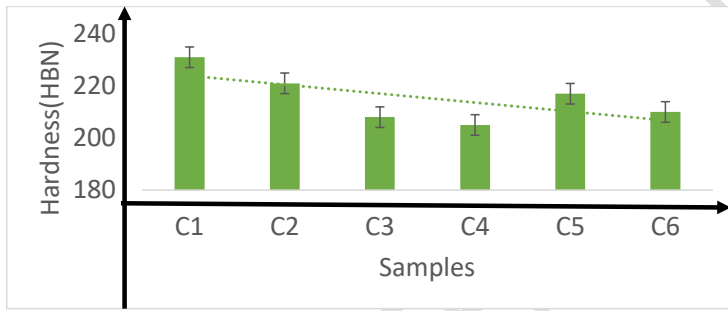


Figure 4: Variation of Hardness with produced samples C

3.4 Tensile

The tensile test results for the CGI produced samples C1-C6 are show in Figure 5. The following was deducted from the graph. C4 has the highest ultimate tensile strength (UTS) value of 1.6 megapascal (MPa) and C3 has the lowest UTS value of 0.2 MPa. While C, C2, C5 and C6 has UTS value of 1.1 MPa ,0.9 MPa, 1.1 MPa and 0.6 MPa respectively.

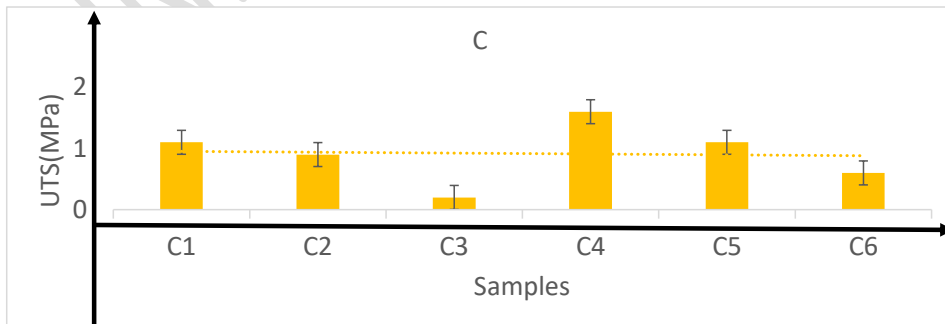


Figure 5: Variation of UTS for Samples C.

3.5 Ductility

Ductility is a measure of the degree of plastic deformation that has been sustained at fracture [30]. A material that exhibit little or no ductility at fracture is said to be brittle [31]. Exhaust system materials are expected to have elements of ductility so as to prevent sudden failure due to impact on the ground [32]. Figure 6 show that C4 and C5 ductility 600% and 401% is the highest in the produced samples. It can be deduced that C4 has the highest ductility of 600 % in C series due to magnesium that was added to aid the transformations α -ferritic microstructure over pearlite phase which is in line with [33] and it is expected that ductile cast iron should have ductility close to that of steels [34]

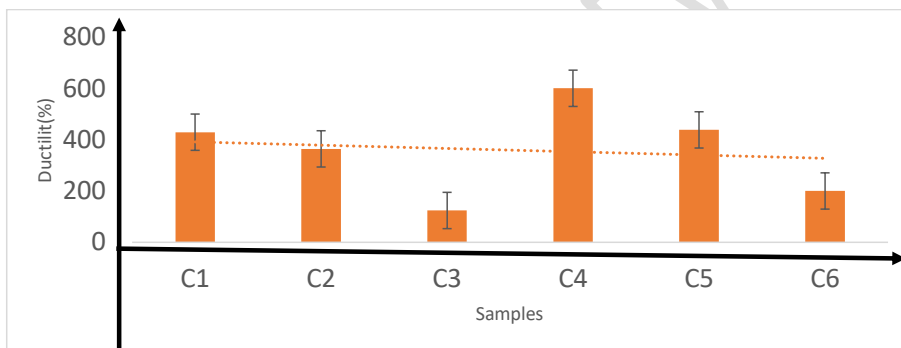


Figure 6: Variation of Ductility with Samples C

3.6 Impact

The result from Figure 7, shows that, the impact strength of the as cast samples C. Figure 4 reveals, that sample C 1 has the highest impact strength of 42.84 J/mm^2 for the series. Which is normal because of surface hardening and presence of copper and silicon in line with [35]. However, the differences in the impact strength are not much for the series C It can be seen clearly that the differences in series C3, C4 are not that much because of the little variance in

pearlitic and ferritic phase. These sets are of series are ideal and suitable for exhaust system outer body parts production according to [36].)

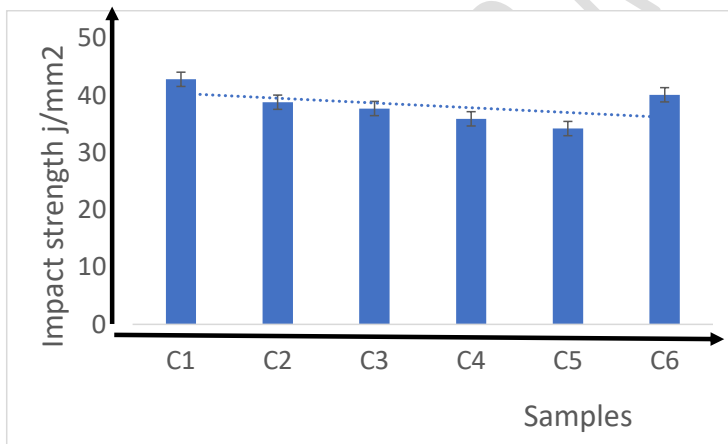


Figure 7: Variation of Impact test with Samples C

4. Conclusions

1. Theoretical and practical failure analysis was carried out on some selected/available exhaust system material parts and it was discovered that the available exhaust system parts are of made up of low and medium carbon steel with the addition of alloying elements which were majorly chromium, aluminum and nickel. Failures occur majorly due to impact of exhaust pipe with

rough and undulated ground and corrosion of exhaust system parts which arises as a result of undue exposure to unfavorable environmental conditions and thermal cycling.

2 Six different CGI was produced from locally sourced materials with varying microstructure tagged C1, C2, C3, C4, C5, and C6 based on the failure analysis that was carried out.

3 Results from the microstructural analysis shown that CGI was produce with C1 and C2 having a microstructure close to gray cast irons, C3 and C4 are pure CGI and C5 and C6 has a structure close to ductile cast iron structure.

4 It can be deduced from the mechanical test results, 240HBN and 204HBN for C1 and C4 are the maximum and minimum hardness values respectively in the produced samples. While 1.5MPa and 600% for C4 are the highest values for tensile strength and ductility result respectively. The difference in the impact resistance from C1 to C6 is not much (C1 is 42.2J/mm², C5 is 34.2J/mm²), C4 value of 35.9J/mm² is an accepted standard in the production of exhaust system materials inline with [37] .

5 Having carried the research work, it is concluded that the CGI produced is suitable for the production of exhaust system parts with C4 being adapted because of its unique mechanical properties, follow by C5.

REFERENCE

- [1] A. Behera and S. C. Mishra, "A novel material used in automotive industry: compacted graphite iron," *Emerg. Mater. Res.*, vol. 1, no. 5, pp. 271–274, 2012, doi: 10.1680/emr.12.00002.
- [2] C. Fragassa, N. Radovic, A. Pavlovic, and G. Minak, "Tribology in Industry Comparison of Mechanical Properties in Compacted and Spheroidal Graphite Irons," vol. 38, no. 1, pp. 45–56, 2016.
- [3] Collini L etal, *peralite gray cast*. 2015.
- [4] S. Dawson and T. Schroeder, "Compacted Graphite Iron : A Viable Alternative," 2000.

- [5] J. C. Sturm and G. Busch, "Cast iron - A predictable material," *China Foundry*, vol. 8, no. 1, pp. 51–61, 2011.
- [6] H. Megahed, E. El-Kashif, A. Y. Shash, and M. A. Essam, "Effect of holding time, thickness and heat treatment on microstructure and mechanical properties of compacted graphite cast iron," *J. Mater. Res. Technol.*, vol. 8, no. 1, pp. 1188–1196, 2019, doi: 10.1016/j.jmrt.2018.07.021.
- [7] M. Sangeetha, S. Prakash, and E. R. N. Sai Kumar, "Improved efficiency in IC engines using proposed design of aqua silencer," *Int. J. Ambient Energy*, vol. 42, no. 4, pp. 389–392, 2021, doi: 10.1080/01430750.2018.1531265.
- [8] X. song Wang and W. zheng Zhang, "Oxidation and Thermal Cracking Behavior of Compacted Graphite Iron under High Temperature and Thermal Shock," *Oxid. Met.*, vol. 87, no. 1–2, pp. 179–188, 2017, doi: 10.1007/s11085-016-9664-6.
- [9] P. Yadav and P. Kothmire, "Exhaust system of commercial vehicle: a review," *IOP Conf. Ser. Mater. Sci. Eng.*, vol. 1116, no. 1, p. 012109, 2021, doi: 10.1088/1757-899x/1116/1/012109.
- [10] A. M. Siregar, C. A. Siregar, and M. Yani, "Engineering of motorcycle exhaust gases to reduce air pollution," *IOP Conf. Ser. Mater. Sci. Eng.*, vol. 821, no. 1, 2020, doi: 10.1088/1757-899X/821/1/012048.
- [11] B. Mohamad, J. Karoly, A. Zelentsov, and S. Amroune, "A hybrid method technique for design and optimization of formula race car exhaust muffler," *Int. Rev. Appl. Sci. Eng.*, vol. 11, no. 2, pp. 174–180, 2020, doi: 10.1556/1848.2020.20048.
- [12] P. Srinivas, V. Mamilla, G. Rao, and S. Moin Ahmed, "Design and Analysis of an Automobile Exhaust Muffler," *Ind. Syst. Eng.*, vol. 1, pp. 10–15, Jan. 2016.
- [13] L. S. Moses, M. T. A. Rahman, A. H. Adom, M. R. M. Jamir, M. A. H. M. Nawi, and M. H. Basha, "An Analysis of The Material and Design of an Exhaust Manifold for A Single-Cylinder Internal Combustion Engine," *J. Adv. Res. Appl. Sci. Eng. Technol.*, vol. 30, no. 2, pp. 163–175, 2023, doi: 10.37934/araset.30.2.163175.
- [14] B. Giechaskiel, A. Melas, G. Martini, and P. Dilara, "Overview of vehicle exhaust particle

- number regulations,” *Processes*, vol. 9, no. 12, pp. 1–24, 2021, doi: 10.3390/pr9122216.
- [15] O. Aranke, W. Algenaid, S. Awe, and S. Joshi, “Coatings for automotive gray cast iron brake discs: A review,” *Coatings*, vol. 9, no. 9, 2019, doi: 10.3390/coatings9090552.
- [16] P. Cunat, “and Other Chromium-Containing Alloys,” pp. 1–24, 2004.
- [17] V. Nayyar, G. Grenmyr, J. Kaminski, and L. Nyborg, “Machinability of compacted graphite iron (CGI) and flake graphite iron (FGI) with coated carbide,” *Int. J. Mach. Mach. Mater.*, vol. 13, no. 1, pp. 67–90, 2013, doi: 10.1504/IJMMM.2013.051909.
- [18] W. L. Guesser, I. Masiero, E. Melleras, and C. S. Cabezas, “Thermal conductivity of gray iron and compacted graphite iron used for cylinder head,” *Rev. Matêria*, vol. 10, no. 2, pp. 265–272, 2005, [Online]. Available: https://www.researchgate.net/publication/283934336_Thermal_conductivity_of_gray_iron_and_compacted_graphite_iron_used_for_cylinder_heads
- [19] A. Oyetunji and A. Opaluwa, “Model development for estimating the aging behaviors of gray cast iron (GCI) alloy at different times and temperatures,” *Int. J. Adv. Manuf. Technol.*, vol. 96, Apr. 2018, doi: 10.1007/s00170-018-1587-8.
- [20] M. Yao, D. Wang, and M. Zhao, “Element Analysis Based on Energy-Dispersive X-Ray Fluorescence,” *Adv. Mater. Sci. Eng.*, vol. 2015, no. 1, pp. 1–7, 2015, doi: 10.1155/2015/290593.
- [21] B. Blakey-Milner *et al.*, “Metal additive manufacturing in aerospace: A review,” *Mater. Des.*, vol. 209, p. 110008, 2021, doi: 10.1016/j.matdes.2021.110008.
- [22] A. Sharma and S. K. Goel, “Materials Science & Engineering A Effect of heat treatment on microstructure , mechanical properties and erosion resistance of cast 23-8-N nitronic steel,” *Mater. Sci. Eng. A*, vol. 637, pp. 56–62, 2015, doi: 10.1016/j.msea.2015.04.031.
- [23] E. Abbasi, Q. Luo, and D. Owens, “A comparison of microstructure and mechanical properties of low-alloy-medium-carbon steels after quench-hardening,” *Mater. Sci. Eng. A*, vol. 725, pp. 65–75, 2018, doi: 10.1016/j.msea.2018.04.012.
- [24] D. Folorunso and S. Bello, “Enhancement of the Mechanical and Thermal Integrity of

- Ijapo Clay for Thermal Insulation,” *J. Environ. Technol.*, vol. 2, no. 1, pp. 30–38, 2021.
- [25] D. W. Hetzner, “Microindentation hardness testing of materials using ASTM E384,” *Microsc. Microanal.*, vol. 9, no. SUPPL. 2, pp. 708–709, 2003, doi: 10.1017/s1431927603443547.
- [26] L. N. García, A. J. Tolley, F. D. Carazo, and R. E. Boeri, “Identification of Cu-rich precipitates in pearlitic spheroidal graphite cast irons,” *Mater. Sci. Technol. (United Kingdom)*, vol. 35, no. 18, pp. 2252–2258, 2019, doi: 10.1080/02670836.2019.1668999.
- [27] T. S. Tshephe, S. O. Akinwamide, E. Olevsky, and P. A. Olubambi, “Additive manufacturing of titanium-based alloys- A review of methods, properties, challenges, and prospects,” *Heliyon*, vol. 8, no. 3, p. e09041, 2022, doi: 10.1016/j.heliyon.2022.e09041.
- [28] B. Bauer, I. Mihalic Pokopec, M. Petrič, and P. Mrvar, “Effect of Cooling Rate on Graphite Morphology and Mechanical Properties in High-Silicon Ductile Iron Castings,” *Int. J. Met.*, vol. 14, no. 3, pp. 809–815, 2020, doi: 10.1007/s40962-020-00432-3.
- [29] S. Upadhyay and K. K. Saxena, “Materials Today : Proceedings Effect of Cu and Mo addition on mechanical properties and microstructure of grey cast iron : An overview,” *Mater. Today Proc.*, no. xxxx, 2020, doi: 10.1016/j.matpr.2020.02.524.
- [30] W. Sckudlarek, M. N. Krmasha, K. S. Al-Rubaie, O. Preti, J. C. G. Milan, and C. E. Da Costa, “Effect of austempering temperature on microstructure and mechanical properties of ductile cast iron modified by niobium,” *J. Mater. Res. Technol.*, vol. 12, pp. 2414–2425, 2021, doi: 10.1016/j.jmrt.2021.04.041.
- [31] E. S. V. Marques, F. J. G. Silva, O. C. Paiva, and A. B. Pereira, “Improving the mechanical strength of ductile cast iron welded joints using different heat treatments,” *Materials (Basel)*, vol. 12, no. 14, 2019, doi: 10.3390/ma12142263.
- [32] E. E. Osakue, L. Anetor, and K. Harris, “Pitting Strength Estimate for Cast Iron and Copper Alloy Materials,” *FME Trans.*, vol. 49, no. 2, pp. 269–279, 2021, doi: 10.5937/fme2102269O.
- [33] C. Bellini, V. Di Cocco, G. Favaro, F. Iacoviello, and L. Sorrentino, “Ductile cast irons: Microstructure influence on the fatigue initiation mechanisms,” *Fatigue Fract. Eng.*

Mater. Struct., vol. 42, no. 9, pp. 2172–2182, 2019, doi: 10.1111/ffe.13100.

- [34] T. Ikeda, N. A. Noda, and Y. Sano, “Conditions for notch strength to be higher than static tensile strength in high-strength ductile cast iron,” *Eng. Fract. Mech.*, vol. 206, no. November 2018, pp. 75–88, 2019, doi: 10.1016/j.engfracmech.2018.11.034.
- [35] M. Górny, G. Angella, E. Tyrała, M. Kawalec, S. Paż, and A. Kmita, “Role of Austenitization Temperature on Structure Homogeneity and Transformation Kinetics in Austempered Ductile Iron,” *Met. Mater. Int.*, vol. 25, no. 4, pp. 956–965, 2019, doi: 10.1007/s12540-019-00245-y.
- [36] B. Kucharska and O. Moraczyński, “Exhaust system piping made by hydroforming: relations between stresses, microstructure, mechanical properties and surface,” *Arch. Civ. Mech. Eng.*, vol. 20, no. 4, pp. 1–11, 2020, doi: 10.1007/s43452-020-00142-x.
- [37] P. Matteis, G. Scavino, A. Castello, and D. Firrao, “High Temperature Fatigue Properties of a Si-Mo Ductile Cast Iron,” *Procedia Mater. Sci.*, vol. 3, pp. 2154–2159, 2014, doi: 10.1016/j.mspro.2014.06.349.